

## THE CONTINUOUS RADIATION OF BRIGHT B3 V STARS\*

KEIICHI KODAIRA†

Mount Wilson and Palomar Observatories, Carnegie Institution of Washington,  
 California Institute of Technology

Received 1969 July 14; revised 1969 July 28

### ABSTRACT

Spectrophotometry from  $\lambda 3297$  to  $\lambda 7850$  is presented for twenty-seven B3 V stars brighter than 5.6 mag in the northern sky. No serious discrepancy is found between the observed and theoretical continua when a model atmosphere of  $T_e = 9600^\circ \text{K}$  and  $\log g = 4.0$ , calculated by Mihalas, is adopted for the primary standard  $\alpha$  Lyr, according to the system of Oke. Apparent effective temperatures are determined for the stars in this program by comparing the colors and Balmer jumps with those of model atmospheres. Most of the observed B3 V stars are found to have an effective temperature between  $16000^\circ$  and  $18000^\circ \text{K}$ .

We discuss an excessively large Balmer jump observed for some rapidly rotating stars, with special attention to the effect of rotation on the fluxes.

### I. INTRODUCTION

Spectrophotometric observations of the continuous radiation of twenty-seven bright B3 V stars were made to determine their *apparent* effective temperatures. This investigation is the first of future studies of the atmospheric structure and chemical composition of selected bright B3 V stars.

Early B-type stars are characterized, on the average, by a high rotation. The conventional criteria for estimating the temperature are often useless for these stars; the profiles of Balmer lines are deformed, and the strong rotational broadening makes it impossible to measure precise intensities of those lines that provide information about the ionization equilibrium. The observed colors of early B-type stars are mostly influenced by interstellar reddening and provide no direct information about the temperature. The most specific and reliable criteria are (1) the total absorption of strong temperature-sensitive lines and (2) the Balmer jump. The former is still affected by the chemical composition. The latter criterion (BJ) is utilized in the present investigation, together with the colors corrected for interstellar reddening.

The rapid rotation, however, affects the structure of the star and consequently complicates the interpretation of the observed data. Since the pioneer work by Sweet and Roy (1953), a series of theoretical papers has been devoted to this problem (see Hardorp and Strittmatter 1968*a, b*). The rotational effect was first observationally confirmed by Guthrie (1963), for B stars that are members of clusters, by finding a statistical correlation between the projected rotational velocity  $v \sin i$  and the excess in  $\beta$ -index. This type of statistical work on cluster members was extended by Kraft and Wrubel (1965), Strittmatter (1966), and Strittmatter and Sargent (1966) to stars of spectral types later than B. Nevertheless, the practical application of the theory to spectroscopic analyses of individual bright stars is highly limited, because the predicted rotational effects cannot be clearly distinguished from genuine differences in intrinsic parameters.

In the present paper, the *apparent* effective temperatures are derived from the observed data by equating the continuous radiation from the rotating stars with that of the static stars. We discuss the discrepancy among the apparent temperatures derived

\* This research was supported by the U.S. Air Force under grant AFOSR 68-1401, monitored by the Air Force Office of Scientific Research of the Office of Aerospace Research.

† On leave from Tokyo Observatory, University of Tokyo.

from different characteristics of the continuous radiation, with special attention paid to the rotational effects. Analyses of high-dispersion spectra, applying the temperatures obtained here, will be given elsewhere (Kodaira and Scholz 1970).

## II. OBSERVATIONS

Twenty-seven B3 V stars brighter than  $m_V = 5.6$  mag were observed with the Cassegrain scanner of the 60-inch reflector at Mount Wilson in 1968. The observations cover all B3 V stars of  $\delta \geq -16^\circ$  listed in the catalog of rotational velocities by Slettebak and Howard (1955), except for a visual triple system,  $\beta$  Mon, and five spectroscopic binaries in the fifth *Lick Spectroscopic Binary Catalogue* (Moore and Neubauer 1948). The star

TABLE 1  
PROGRAM STARS

No.	Name	HD	$V^*$	$B-V^*$	$U-B$	Remarks
1.....	35 Ari	16908	4.67	-0.13	-0.63	Cas-Tau group
2.....	29 Per	20365	5.15	-0.06	-0.56	$\alpha$ Peg group
3.....	HR 1034	21278	4.98	-0.10	-0.56	$\alpha$ Peg group
4.....	29 Tau	23466	5.34	-0.11	-0.61	Cas-Tau group
5.....	30 Tau	23793	5.00			Cas-Tau group
6.....	40 Tau	25558	5.33	-0.08	-0.56	Cas-Tau group
7.....	48 Per	25940	4.03	-0.03	-0.55	Cas-Tau group, Bep
8.....	$\mu$ Tau	26912	4.30	-0.05	-0.51	
9.....	$\eta$ Aur	32630	3.18	-0.18	-0.67	Cas-Tau group
10.....	114 Tau	35708	4.89	-0.14	-0.77	Cas-Tau group
11.....	121 Tau	36819	5.16			Cas-Tau group
12.....	$\xi$ Ori	42560	4.48	-0.17	-0.66	Cas-Tau group
13.....	HR 2825	58343	5.33	-0.04		Be
14.....	$\eta$ Hya	74280	4.30	-0.20	-0.74	
15.....	$\eta$ UMa	120315	1.86	-0.19	-0.67	Cas-Tau group
16.....	$\iota$ Her	160762	3.80	-0.18	-0.69	
17.....	96 Her	164852	5.10	-0.10		
18.....	HR 7210	177003	5.16			
19.....	12 Vul	187811	4.96	-0.12	-0.68	Be
20.....	25 Cyg	189687	5.20	-0.17		Be
21.....	17 Vul	190993	4.96			
22.....	28 Cyg	191610	4.92	-0.12	-0.78	Be
23.....	HR 7739	192685	4.77	-0.18	-0.73	
24.....	6 Cep	203467	5.14	-0.02		
25.....	70 Cyg	204403	5.21			
26.....	$\pi^1$ Cyg	206672	4.67	-0.12	-0.69	
27.....	16 Peg	208057	5.07	-0.18		

\* The values for stars without  $U - B$  data are adopted from Hoffleit (1964); others from Johnson *et al.* (1966).

28 Cyg was included in our program because the calculated binary orbit shows a discrepancy among the observed data. A list of the program stars is given in Table 1. Scanning was performed according to the system established by Oke (1964) over the region  $\lambda\lambda 3290-7850$ . The bandwidth was 25 Å for  $\lambda\lambda 3290-5840$ , while 50 Å was used for  $\lambda\lambda 5255-7850$  ( $\lambda\lambda 5255-5840$  overlapped) as in Oke's original system. The effect of the different bandwidth was empirically investigated for Oke's secondary standard stars. In some secondary standards of spectral type earlier than B5, strong He I lines fall in the 50 Å bands  $\lambda\lambda 3571, 4032, \text{ and } 4464$ , and affect the monochromatic magnitudes at these wavelengths by  $\delta m = 0.010, 0.014, \text{ and } 0.014$ , respectively. As more than three of the secondary standards were referred to each night, the effect upon the final results was found to be less than 0.007 mag. The integration time of 10 seconds was chosen in order to secure the integrated photon count of  $2 \times 10^4$  or more for all observed bands except

at the longest and shortest wavelengths. Winter stars were observed in 1968 January and October, and summer stars in 1968 August, September, and October. Observations of the red and near-infrared region for all program stars were made in 1968 September and October. In order to check the month-to-month effect, some of the objects were observed over the two succeeding runs. The systematic month-to-month effect, as well as the systematic night-to-night effect, proved to be less than  $\pm 0.015$  mag.

The observed monochromatic magnitudes,  $m(1/\lambda) = -2.5 \log F(1/\lambda) + C$ , are given in Table 2. The primary standard,  $\alpha$  Lyr, was normalized to the blanketed model of  $T_e = 9600^\circ$  K and  $\log g = 4.0$  given by Mihalas (1966), for various reasons discussed in the next section. The constant  $C$ , above, was so determined that our absolute system gives the same value as Oke's original system for  $\lambda 5000$ . The accuracy of the given data is estimated to be  $\pm 0.010$  mag for  $\lambda > 4032$  and  $\pm 0.015$  mag for  $\lambda < 4032$  within our

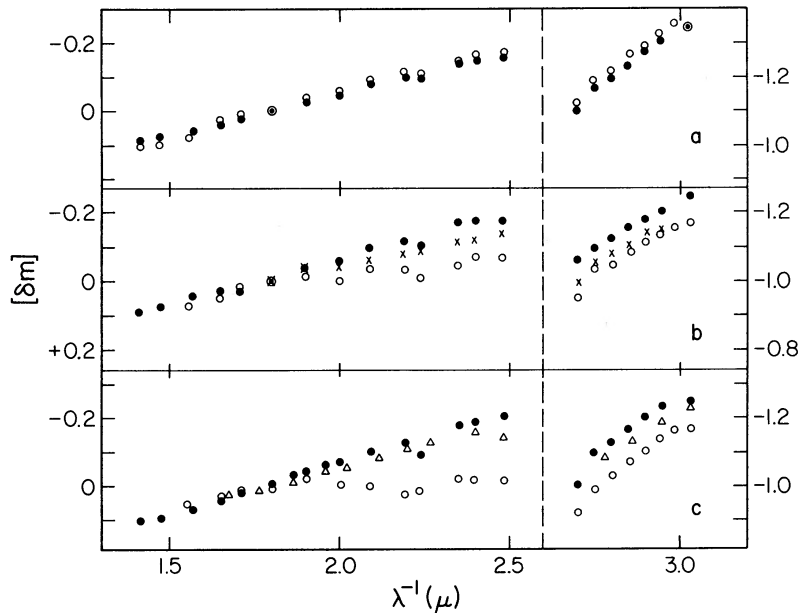


FIG. 1.—Comparison of different observational systems. (a)  $\eta$  Hya, (b)  $\iota$  Her, (c)  $\eta$  UMa.  $[\delta m] = \delta m(*) - \delta m(\alpha \text{ Lyr})$ . Left scale is for  $1/\lambda < 2.6$ ; right scale, for  $1/\lambda > 2.6$ . Dots, present data; circles, Wolff *et al.*; crosses, Jugaku and Sargent; triangles, Bahner.

observational system, except for  $\lambda\lambda 3290, 3704, 4032,$  and  $7850$ , where the probable error may reach  $\pm 0.025$  mag.

#### a) Comparison with Other Sources

One of the secondary standard stars, B3 V star  $\eta$  Hya, was also observed by Wolff, Kuhi, and Hayes (1968). Figure 1, *a*, shows the comparison between their result and ours. To avoid the discrepancy arising from the different method of absolute calibration, the difference

$$[\delta m] = \delta m(*) - \delta m(\alpha \text{ Lyr})$$

is plotted, where

$$\delta m = m(1/\lambda) - m(1/\lambda = 1.8).$$

The discrepancy is less than 0.015 mag for  $\lambda\lambda 4032$ –6800 and about 0.03 mag for  $\lambda\lambda 4032$  and 6800; the coincidence is good, although the points by Wolff *et al.* (1968) are located higher than ours, and increase in height toward the ultraviolet. This tendency is re-

TABLE 2  
MONOCHROMATIC MAGNITUDES

$\lambda$ (Å)	$1/\lambda$ ( $\mu$ )	Corr.*	1	2	3	4	5	6	7	8	9	10	11	12	13	14
3297	3.033	0.07	4.79	5.49	5.31	5.54	5.19	5.46	4.40	4.57	3.20	4.80	5.51	4.51	5.10	4.16
3390	2.950	0.06	4.78	5.45	5.27	5.50	5.18	5.45	4.36	4.55	3.18	4.79	5.49	4.47	5.08	4.17
3448	2.900	0.06	4.78	5.44	5.28	5.50	5.19	5.49	4.35	4.55	3.20	4.81	5.48	4.49	5.09	4.18
3509	2.850	0.06	4.79	5.44	5.28	5.51	5.20	5.50	4.34	4.56	3.20	4.81	5.54	4.50	5.08	4.20
3571	2.800	0.06	4.79	5.43	5.28	5.52	5.20	5.50	4.32	4.55	3.20	4.82	5.54	4.51	5.07	4.22
3636	2.750	0.06	4.80	5.43	5.28	5.52	5.21	5.50	4.32	4.55	3.21	4.84	5.53	4.52	5.06	4.23
3704	2.700	0.06	4.91	5.48	5.29	5.53	5.26	5.56	4.38	4.57	3.26	4.91	5.60	4.58	5.19	4.27
4032	2.480	-0.05	4.32	4.92	4.72	5.08	4.67	5.04	3.81	3.99	2.75	4.54	5.06	4.06	4.81	3.87
4167	2.402	-0.04	4.32	4.92	4.73	5.06	4.73	5.03	3.81	4.02	2.75	4.55	5.08	4.09	4.82	3.91
4255	2.350	-0.04	4.36	4.93	4.76	5.09	4.75	5.05	3.82	4.03	2.77	4.57	5.11	4.11	4.83	3.93
4464	2.240	-0.03	4.44	5.02	4.83	5.13	4.84	5.13	3.89	4.10	2.87	4.67	5.20	4.21	4.90	4.02
4566	2.190	-0.02	4.42	4.99	4.82	5.16	4.82	5.12	3.86	4.08	2.86	4.65	5.16	4.20	4.88	4.03
4785	2.090	-0.01	4.46	5.06	4.85	5.19	4.88	5.18	3.92	4.14	2.96	4.72	5.21	4.28	4.91	4.10
5000	2.000	0	4.55	5.09	4.94	5.26	4.95	5.23	3.95	4.19	3.03	4.79	5.25	4.33	4.95	4.17
5255	1.903	0	4.60	5.10	4.96	5.29	4.99	5.25	3.97	4.20	3.08	4.80	5.28	4.38	4.93	4.23
5556	1.800	0.02	4.68	5.16	5.03	5.37	5.07	5.32	4.03	4.26	3.17	4.89	5.35	4.46	4.98	4.32
5840	1.712	0.02	4.74	5.20	5.07	5.40	5.13	5.37	4.07	4.30	3.24	4.94	5.39	4.53	5.00	4.38
6055	1.652	0.03	4.78	5.24	5.12	5.44	5.18	5.41	4.10	4.34	3.31	4.99	5.43	4.58	5.03	4.44
6370	1.570	0.04	4.86	5.30	5.18	5.52	5.25	5.47	4.14	4.40	3.37	5.06	5.48	4.64	5.05	4.51
6800	1.471	0.05	4.95	5.36	5.25	5.58	5.34	5.54	4.19	4.47	3.47	5.15	5.56	4.73	5.08	4.60
7100	1.408	0.06	5.00	5.41	5.31	5.62	5.39	5.58	4.23	4.52	3.54	5.21	5.63	4.78	5.10	4.66
7530	1.328	0.06	5.07	5.48	5.39	5.68	5.46	5.64	4.25	4.60	3.63	5.28	5.66	4.86	5.10	4.73
7850	1.274	0.07	5.06	5.48	5.45	5.75	5.49	5.64	4.30	4.61	3.71	5.33	5.69	4.85	5.13	4.68
$\lambda$ (Å)	$1/\lambda$ ( $\mu$ )	Corr.*	15	16	17	18	19	20	21	22	23	24	25	26	27	
3297	3.033	0.07	1.95	3.83	5.43	5.30	4.92	5.26	5.13	4.96	4.81	5.40	5.45	4.88	5.15	
3390	2.950	0.06	1.93	3.81	5.40	5.31	4.88	5.25	5.11	4.92	4.79	5.35	5.44	4.85	5.12	
3448	2.900	0.06	1.94	3.81	5.41	5.33	4.86	5.25	5.11	4.92	4.78	5.34	5.44	4.84	5.14	
3509	2.850	0.06	1.96	3.81	5.41	5.34	4.85	5.24	5.12	4.91	4.79	5.33	5.43	4.85	5.14	
3571	2.800	0.06	1.97	3.82	5.42	5.34	4.85	5.25	5.12	4.91	4.80	5.32	5.44	4.84	5.14	
3636	2.750	0.06	1.98	3.83	5.43	5.36	4.85	5.26	5.13	4.91	4.81	5.30	5.44	4.85	5.15	
3704	2.700	0.06	2.05	3.84	5.43	5.39	4.94	5.27	5.15	4.97	4.83	5.31	5.45	4.85	5.17	
4032	2.480	-0.05	1.51	3.39	4.97	5.00	4.53	4.86	4.70	4.62	4.42	4.89	4.97	4.40	4.72	
4167	2.402	-0.04	1.55	3.42	4.96	5.01	4.54	4.88	4.71	4.63	4.43	4.90	4.98	4.40	4.72	
4255	2.350	-0.04	1.58	3.44	4.97	5.04	4.55	4.89	4.73	4.65	4.45	4.90	5.00	4.42	4.74	
4464	2.240	-0.03	1.71	3.55	5.05	5.14	4.64	4.97	4.83	4.75	4.56	4.96	5.08	4.51	4.84	
4566	2.190	-0.02	1.68	3.55	5.06	5.14	4.65	4.98	4.84	4.74	4.56	4.95	5.10	4.51	4.84	
4785	2.090	-0.01	1.76	3.62	5.11	5.21	4.71	5.04	4.89	4.81	4.62	4.99	5.16	4.57	4.91	
5000	2.000	0	1.83	3.70	5.18	5.30	4.77	5.10	4.98	4.88	4.69	5.02	5.22	4.63	4.98	
5255	1.903	0	1.90	3.76	5.23	5.37	4.81	5.14	5.03	4.89	4.75	5.00	5.26	4.66	5.03	
5556	1.800	0.02	2.01	3.86	5.30	5.46	4.90	5.23	5.11	5.00	4.84	5.05	5.34	4.74	5.11	
5840	1.712	0.02	2.07	3.93	5.35	5.55	4.95	5.29	5.16	5.04	4.90	5.07	5.39	4.78	5.17	
6055	1.652	0.03	2.13	3.97	5.39	5.59	4.99	5.33	5.23		4.95	5.10	5.44		5.23	
6370	1.570	0.04	2.22	4.04	5.45	5.66	5.05	5.40	5.30		5.03	5.14	5.51		5.30	
6800	1.471	0.05	2.31	4.14	5.54	5.76	5.13	5.49	5.40		5.13	5.19	5.60		5.40	
7100	1.408	0.06	2.36	4.21	5.60	5.83	5.19	5.56	5.47		5.20	5.22	5.68		5.47	
7530	1.328	0.06	2.42	4.33	5.68	5.92	5.25	5.57	5.55		5.29	5.26	5.77		5.58	
7850	1.274	0.07	2.46	4.39	5.66	5.98	5.27	5.63	5.62		5.33	5.28	5.82		5.62	

\*  $\alpha$  Lyr(adopted) =  $\alpha$  Lyr(original) + corr.; corr. for BJ = 0.145.

versed in the case of  $\iota$  Her, as seen in Figure 1, *b*, and the discrepancy is much greater than in the case of  $\eta$  Hya. The continuum of  $\iota$  Her was also scanned by Jugaku and Sargent (1968). Their data fall between ours and those of Wolff *et al.* (1968). The difference appears to be wavelength-dependent. Figure 1, *c*, shows the data for  $\eta$  UMa observed by Wolff *et al.* (1968), by Bahner (1963), and by us. Despite the discrepancy of 0.06 mag at  $\lambda 4032$ , Bahner's result and ours are in general agreement, while the data of Wolff *et al.* (1968) deviate by a surprising amount from the other two systems in the photographic region. As no observation of variability as large as 0.1 mag was reported for these bright stars, the discrepancy might have arisen from an insufficient correction for the atmospheric extinction, or from the nonlinear characteristics of the observational equipment, or for both reasons. A comparison of scan data with *UBV* data (Johnson *et al.* 1966) suggests that the present system is definitely superior to that of Wolff *et al.* (1968), at least concerning the B3 stars shown in Figure 1. It should be noted that the different systems give nearly identical Balmer jumps in spite of the discrepancy.

### III. THE CONTINUOUS SPECTRUM

#### *a) Absolute Calibration*

The interpretation of the observed continua depends on the absolute calibration of the primary standard star  $\alpha$  Lyr. Oke's original system is based on a model of  $\alpha$  Lyr

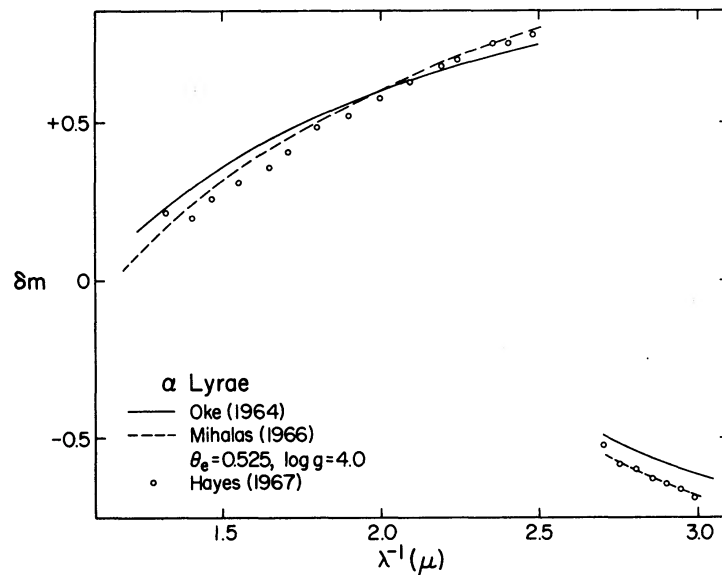


FIG. 2.—Comparison of different absolute calibrations of  $\alpha$  Lyr

corresponding to an unblanketed model atmosphere for  $T_e = 9500^\circ$  K and  $\log g = 4.44$  calculated by Mihalas (1965). Hayes (1967) made an absolute calibration of the continuous radiation of  $\alpha$  Lyr, which justified the suspicion of a larger Balmer jump for this star ( $BJ = 1.43$ , cf. Bahner 1963; Whiteoak 1966) than that in the original model ( $BJ = 1.28$ ). The Paschen continuum was found by Hayes (1967) to be steeper than that originally adopted. In Figure 2, Hayes's continuum is compared with those of the original *unblanketed* model of  $\alpha$  Lyr, and of the *blanketed* model for  $T_e = 9600^\circ$  K and  $\log g = 4.0$  calculated by Mihalas (1966). Hayes's data fit the blanketed model well for  $T_e = 10000^\circ$  K, as suggested by Wolff *et al.* (1968), and  $\log g = 3.6$ , as found by Heintze (1968). Calculations by Hardorp and Scholz (1968), however, led to the conclusion that the different observed characteristics of  $\alpha$  Lyr find optimal match with a blanketed model for  $T_e = 9700^\circ$  K and  $\log g = 3.9$ . Figure 2 shows that this choice is still com-

patible with Hayes's data. The present data in Table 2 are all calibrated with a blanketed model of  $\alpha$  Lyr with  $T_e = 9600^\circ$  K ( $\theta_e = 0.525$ ) and  $\log g = 4.0$ , as suggested by Mihalas (1966). The corrections from Oke's system to the present one are given in Table 2. The effect of the absorption lines has been studied by Baschek and Oke (1965). Their result shows a nearly homogeneous blocking of  $\delta m \simeq 0.01$  for  $\lambda < 5000 \text{ \AA}$ , whose influence is negligible in the discussion below.

*b) Balmer Jump and Colors*

Based on the above calibration, the Balmer jump (BJ) was graphically determined as the difference in the monochromatic magnitude at  $1/\lambda = 2.70$  between the Paschen

TABLE 3  
COLORS AND BALMER JUMP

No.	Name	X	Y	Z	BJ	$X_0$	$Y_0$	$Z_0$
1....	35 Ari	0.37	0.26	0.32	0.61	+0.32	0.31	0.37
2....	29 Per	0.44	0.17	0.25	0.60	+0.29	0.31	0.39
3....	HR 1034	0.46	0.21	0.28	0.69	+0.36	0.305	0.375
4....	29 Tau	0.36	0.21	0.25	0.60	+0.25	0.315	0.355
5....	30 Tau	0.38	0.25	0.32	0.63	+0.32	0.31	0.38
6....	40 Tau	0.38	0.20	0.26	0.58	+0.26	0.315	0.375
7....	48 Per	0.46	0.17	0.20	0.60	+0.31	0.31	0.34
8....	$\mu$ Tau	0.47	0.18	0.26	0.65	+0.34	0.305	0.385
9....	$\eta$ Aur	0.34	0.31	0.37	0.66	+0.34	0.31	0.37
10....	114 Tau	0.17	0.24	0.32	0.45	+0.07	0.34	0.42
11....	121 Tau	0.38	0.19	0.27	0.56	+0.25	0.315	0.395
12....	$\xi$ Ori	0.31	0.26	0.32	0.62	+0.25	0.32	0.375
13....	HR 2825	0.19	0.10	0.12	0.29	-0.08	0.375	0.395
14....	$\eta$ Hya	0.19	0.29	0.34	0.52	+0.15	0.33	0.38
15....	$\eta$ UMa	0.29	0.33	0.35	0.63	+0.29	0.325	0.35
16....	$\iota$ Her	0.27	0.31	0.35	0.60	+0.27	0.31	0.35
17....	96 Her	0.36	0.24	0.30	0.60	+0.28	0.315	0.375
18....	HR 7210	0.20	0.32	0.37	0.56	+0.20	0.32	0.37
19....	12 Vul	0.20	0.25	0.29	0.46	+0.11	0.335	0.375
20....	25 Cyg	0.27	0.25	0.33	0.55	+0.19	0.325	0.405
21....	17 Vul	0.28	0.27	0.36	0.62	+0.23	0.32	0.41
22....	28 Cyg	0.17	0.26	...	0.43	+0.09	0.335	...
23....	HR 7739	0.24	0.28	0.36	0.59	+0.20	0.32	0.40
24....	6 Cep	0.37	0.10	0.17	0.47	+0.13	0.33	0.40
25....	70 Cyg	0.34	0.24	0.34	0.62	+0.26	0.315	0.415
26....	$\pi^1$ Cyg	0.33	0.23	...	0.58	+0.23	0.32	...
27....	16 Peg	0.30	0.27	0.36	0.62	+0.25	0.32	0.405

continuum and the extrapolated Balmer continuum. Since the observed continua of B3 V stars are smooth and barely curved, we find an accuracy of  $\delta \text{BJ} = \pm 0.02$ . The measured BJ's are given in Table 3. Let us introduce color indices  $X$ ,  $Y$ , and  $Z$  to treat the characteristics of the continuum quantitatively:

$$X = m(1/\lambda = 2.80) - m(1/\lambda = 2.19),$$

$$Y = m(1/\lambda = 1.80) - m(1/\lambda = 2.19),$$

$$Z = m(1/\lambda = 1.41) - m(1/\lambda = 1.80).$$

The wavelengths  $1/\lambda = 1.41, 1.80, 2.19$ , and  $2.80$  were selected because 25  $\text{\AA}$  bands centered at these positions are most free from absorption lines. The quantities are given in Table 3 and plotted in Figures 3 and 4 as  $(X, Y)$ - and  $(Y, Z)$ -diagrams. The quantities  $X$  and  $Y$

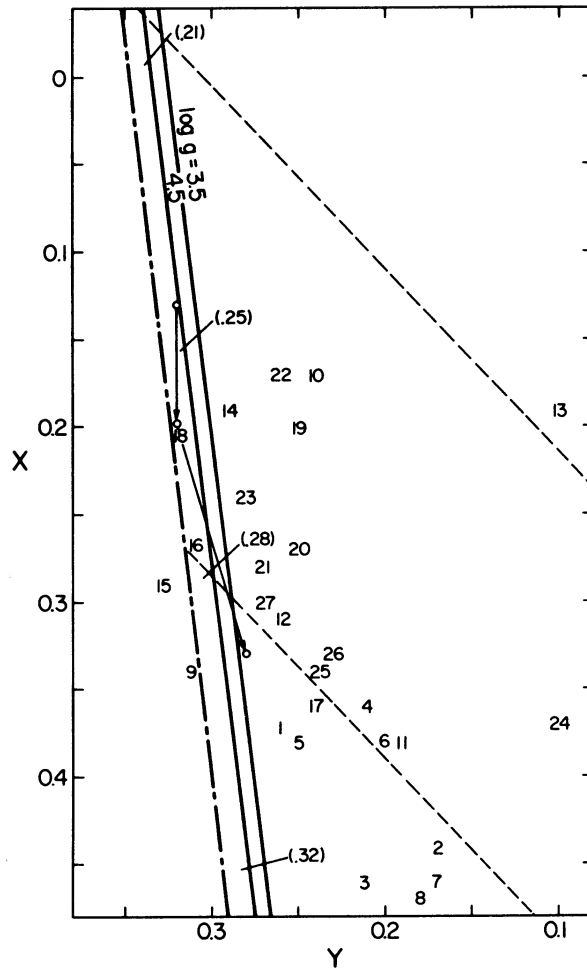


FIG. 3.—The  $(X, Y)$ -diagram:  $X = m(1/\lambda = 2.80) - m(1/\lambda = 2.19)$ ;  $Y = m(1/\lambda = 1.80) - m(1/\lambda = 2.19)$ . *Straight lines*, theoretical values from Mihalas (1965), with  $\theta_0$  in parentheses. *Heavy broken line*, the empirical standard line (see text). *Broken lines*, reddening lines  $\delta X = -1.05 \delta Y$ . Arrows show the rotational effect for a star of  $5.36 M_{\odot}$ , at the breakup velocity, pointing from zero rotation to pole-on, and from pole-on to equator-on case.

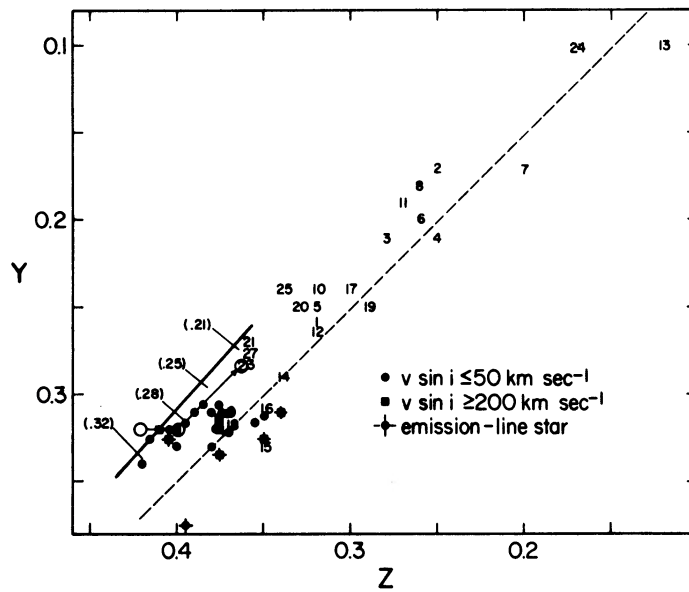


FIG. 4.— $(Y, Z)$ -diagram:  $Y = m(1/\lambda = 1.80) - m(1/\lambda = 2.19)$ ;  $Z = m(1/\lambda = 1.41) - m(1/\lambda = 1.80)$ . *Straight line*, theoretical values from Mihalas, with  $\theta_0$  in parentheses. *Broken line*, reddening line  $\delta Y = +1.00 \delta Z$ . Circles and arrows show the theoretical rotational effect as in Fig. 3. *Dots*, intrinsic positions  $(Y_0, Z_0)$ .

in our system have the following approximate relations to  $U - B$  and  $B - V$  for unreddened main-sequence A and B stars:

$$X = 1.540 (U - B) + 1.31 \pm 0.03 ,$$

$$Y = -0.700 (B - V) + 0.18 \pm 0.02 .$$

The unreddened standard stars fall on a line with a scatter of  $\delta Y = \pm 0.01$  in the  $(X, Y)$ -diagram. The portion of this line near B3 V stars is illustrated in Figure 3 and is compared with the theoretical curves corresponding to the unblanketed models by Mihalas (1965). The empirical curve runs parallel to the theoretical curves but is slightly shifted by  $\delta Y = 0.02$  toward the blue. As the variation of the Paschen continuum is small for the temperatures in question,  $(Y, Z)$ -curves can provide no criterion for a determination of the temperature. The correction of the interstellar reddening was made according to Whitford (1958), including the small deviation from the  $1/\lambda$  law. The reddening lines are

$$\delta X = -1.05 \delta Y$$

and

$$\delta Y = +1.00 \delta Z ,$$

as represented in Figures 3 and 4. In the  $(Y, Z)$ -diagram, the reddening runs nearly parallel to the theoretical  $(Y, Z)$ -curve. The figures show that most of the observed objects are reddened. The *apparent* intrinsic colors  $X_0$ ,  $Y_0$ , and  $Z_0$  are given in Table 2. It is important to note that these colors are based on the single empirical standard line in the  $(X, Y)$ -diagram and therefore are subject to systems-tie correction if the observed stars belong to different groups with standard lines differing because of rotational or age effects. In Figures 4, 5, and 6 the *apparent* intrinsic locations corresponding to values of BJ,  $X_0$ , and  $Y_0$  in Table 3 are compared with the theoretical curves. Five stars—48 Per, HR 2825, 12 Vul, 25 Cyg, and 28 Cyg—are emission-line objects. They follow the general behavior of B3 V stars except for HR 2825, which showed strong emission lines at the time of this observation (1968, middle January). The effect of the emission component will be discussed separately (Kodaira and Scholz 1970).

### c) Temperature

An *apparent* effective temperature can be derived by simply equating the observed quantity with the theoretical one for the static model atmosphere. Table 4 contains *apparent* effective temperatures according to BJ and  $X_0$  for  $\log g = 4.0$ . The temperature derived from  $Y_0$  is not independent of  $\theta_e(X_0)$  because we assumed a single standard line in the  $(X, Y)$ -diagram:

$$\theta_e(X_0) - \theta_e(Y_0) = -0.04 .$$

The difference was introduced through the small offset ( $\delta Y = -0.02$ ) of the steep standard lines in the diagram. A small offset is also observed between the empirical and the theoretical points in the  $(BJ, X_0)$ -diagram, and is the cause of the systematic difference between  $\theta_e(BJ)$  and  $\theta_e(X_0)$ :

$$\theta_e(X_0) \simeq \theta_e(BJ) - 0.005 .$$

The small offsets are, in both cases, of the order of the accuracy of the measurements, and probably of the accuracy of the observational system. The discrepancy between the observed and the theoretical continua for early B stars is no longer as serious as in the preceding attempts by Wolff *et al.* (1968) and Jugaku and Sargent (1968). As a first approximation, one can adopt the temperature of the theoretical point for  $\log g = 4.0$  nearest to the observed point in the  $(BJ, X_0)$ -diagram. The adopted values are tabulated

in Table 4. Our results show that the *apparent* effective temperatures of non-emission-line B3 V stars fall into a narrow range between  $\theta_e = 0.27$  and 0.305, with three hotter exceptions of 114 Tau ( $\theta_e = 0.24$ ), 6 Cep (0.25), and  $\eta$  Hya (0.26).

In the preceding discussion we utilized the unblanketed model atmosphere by Mihalas (1965). Mihalas and Morton (1965) and Adams and Morton (1968) calculated blanketed models for  $\theta_e = 0.23$  and 0.30, and found their atmospheric structures very nearly the same as unblanketed models for  $\theta_e = 0.21$  and 0.285, respectively. When this correction factor for the blanketing effect is taken into account, our temperature scale fits that of Hanbury Brown *et al.* (1967). The adopted temperatures of  $\iota$  Her,  $\eta$  Hya, and

TABLE 4  
TEMPERATURE OF B3 V STARS\*

No.	Name	$\theta_e(\text{BJ})$	$\theta_e(X_0)$	$\theta_e$ (adopt.)	$v \sin i$ (km sec <sup>-1</sup> )	Remarks
1.....	35 Ari	0.295	0.295	0.295	135	
2.....	29 Per	0.285	0.285	0.285	145	
3.....	HR 1034	0.31	0.30	0.305	50	
4.....	29 Tau	0.285	0.275	0.28	145	
5.....	30 Tau	0.295	0.295	0.295	20	
6.....	40 Tau	0.28	0.28	0.28	25	
7.....	48 Per	0.29	0.29	0.29	250	Bep
8.....	$\mu$ Tau	0.30	0.30	0.30	80	
9.....	$\eta$ Aur	0.305	0.30	0.30	125	
10.....	114 Tau	0.245	0.23	0.24	10	
11.....	121 Tau	0.275	0.275	0.275	115	
12.....	$\xi$ Ori	0.29	0.275	0.28	230	$\delta$ BJ large
13.....	HR 2825	(0.19)	(0.19)	...	30	Be
14.....	$\eta$ Hya	0.265	0.25	0.26	135	
15.....	$\eta$ UMa	0.295	0.28	0.28	210	$\delta$ BJ moderate
16.....	$\iota$ Her	0.285	0.28	0.28	0	
17.....	96 Her	0.285	0.28	0.28	220	
18.....	HR 7210	0.28	0.265	0.27	0	
19.....	12 Vul	0.25	0.24	0.245	300	Be
20.....	25 Cyg	0.275	0.26	0.27	230	Be
21.....	17 Vul	0.295	0.27	0.28	240	$\delta$ BJ large
22.....	28 Cyg	0.235	0.235	0.235	310	Be
23.....	HR 7739	0.28	0.265	0.27	275	$\delta$ BJ large
24.....	6 Cep	0.25	0.25	0.25	150	
25.....	70 Cyg	0.295	0.28	0.28	135	$\delta$ BJ moderate
26.....	$\pi^1$ Cyg	0.28	0.27	0.275	120	
27.....	16 Peg	0.295	0.275	0.28	150	$\delta$ BJ large

\* Temperatures given refer to the unblanketed models. The  $\theta$ 's in the blanketed system are larger than these by  $\delta\theta \simeq 0.02$  (see text).

$\eta$  UMa are identical with those proposed by Heintze (1969) when corrected for the blanketing effect. According to Mihalas and Stone (1968), the non-LTE effect on the atmospheric structure of B3 V stars is one-twentieth of the blanketing effect, negligible in the present discussion. It should be emphasized that, while the absolute temperature scale may still be subject to an error arising from the absolute photometric calibration, there is no doubt as to the relative temperature scale of the observed B3 V stars.

#### IV. DISCUSSION

The temperatures presented in the last section refer to the theoretical curve of  $\log g = 4.0$ . The scatter of the observed points in the (BJ,  $X_0$ )-diagram, however, is more than the gravity effect for a static model atmosphere between  $\log g = 3.5$  and  $\log g = 4.5$ . Before examining the possible gravity effect, it is necessary to estimate the

rotational effect. The  $v \sin i$  of the program stars in Table 4 are from Slettebak and Howard (1955). The theoretical rotational effect in Figures 3–6 was calculated by Har-dorp and Strittmatter (1968*a*). Atmospheres for a star of  $5.36 M_{\odot}$  were used as examples. The rotational effect is nearly equivalent to lowering the effective temperature. The geometrical effects of “pole-on” ( $i = 0^{\circ}$ ) stars slightly increase the surface gravity; those of “equator-on” ( $i = 90^{\circ}$ ) decrease it by as much as  $\delta \log g = 1$ . When we examine the (BJ,  $X_0$ )-diagram, we find an effect from the observed data opposite in sense to that

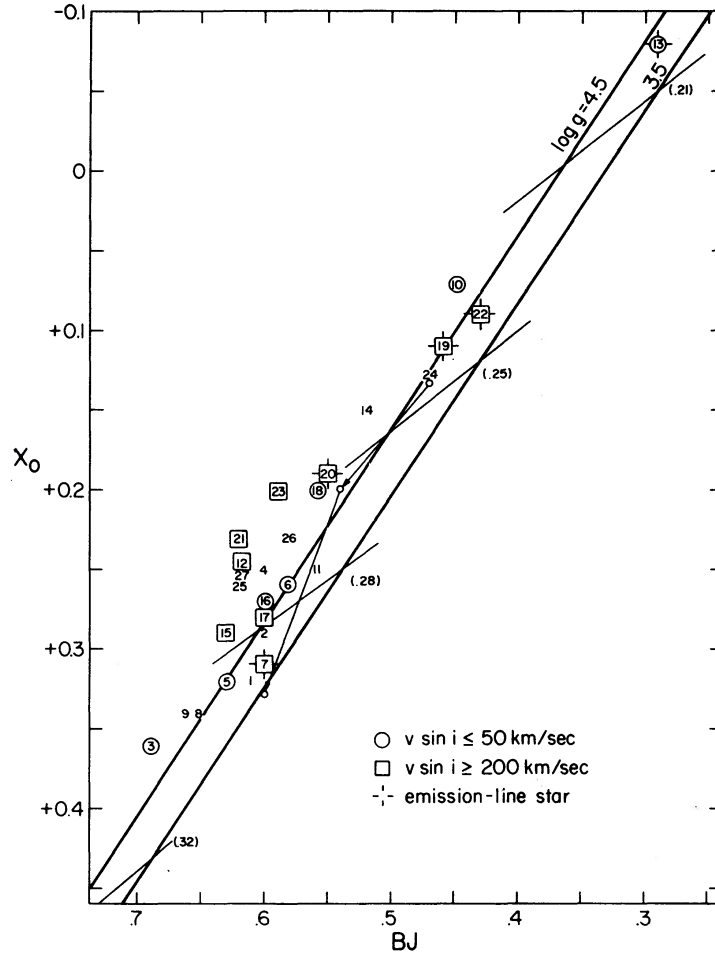


FIG. 5.—(BJ,  $X_0$ )-diagram, where  $X_0$  is the intrinsic color  $X$  corrected for interstellar reddening. Theoretical values of (BJ,  $X_0$ ) and rotational effect, as in Fig. 3.

predicted. The observed effect is represented in Figure 7, the  $[v \sin i, \delta BJ(X_0)]$ -diagram, where  $\delta BJ(X_0)$  is the horizontal shift of the observed point from the theoretical line for  $\log g = 3.5$ . Many observed rapid rotators tend to have too large a BJ for the color  $X_0$ . This contradiction could be resolved by separating the standard lines, according to  $v \sin i$ , in the ( $X$ ,  $Y$ )-diagram. When the standard line is shifted along the  $Y$ -axis by a small amount  $\delta Y < 0$ , it increases the color index  $X_0$  of reddened objects such as most of the observed rapid rotators, consequently decreasing their  $\delta BJ(X_0)$ 's. The theory predicts  $|\delta Y| < 0.03$ , and our data of least-reddened rapid rotators lead to a limit  $|\delta Y| < 0.05$  (see Fig. 3).

To obtain the reversed sense of the effect observed, however, requires a dispersion in the standard lines of  $|\delta Y| \gtrsim 0.07$ , which is compatible neither with the observations

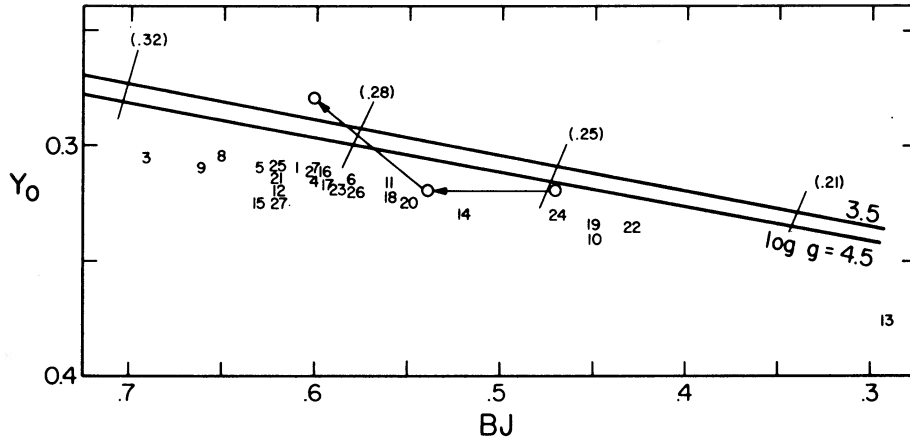


FIG. 6.—(BJ,  $Y_0$ )-diagram, where  $Y_0$  is the intrinsic color  $Y$  corrected for interstellar reddening. Theoretical values of (BJ,  $Y_0$ ) and rotational effect, as in Fig. 3.

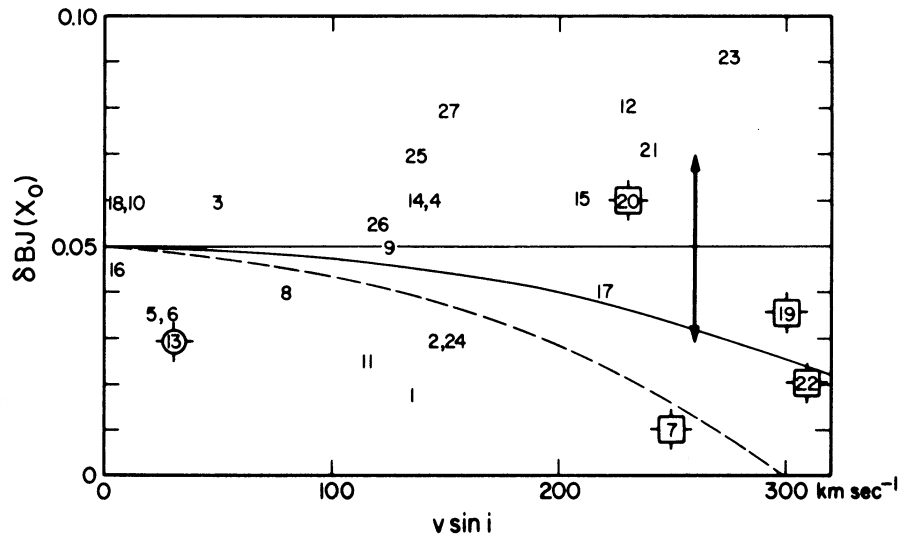


FIG. 7.—Diagram of  $v \sin i$  versus  $\delta BJ(X_0)$ , where  $BJ(X_0)$  is the excess in the BJ relative to the theoretical BJ for  $\log g = 3.5$  and  $X_0$  from the (BJ,  $X_0$ )-diagram;  $v \sin i$  is from Slettebak and Howard. *Solid curve*, theoretical rotational effect; *broken curve*, empirical rotational effect from Guthrie. Vertical line shows the gravity effect on BJ for  $\delta \log g = 1.0$ .

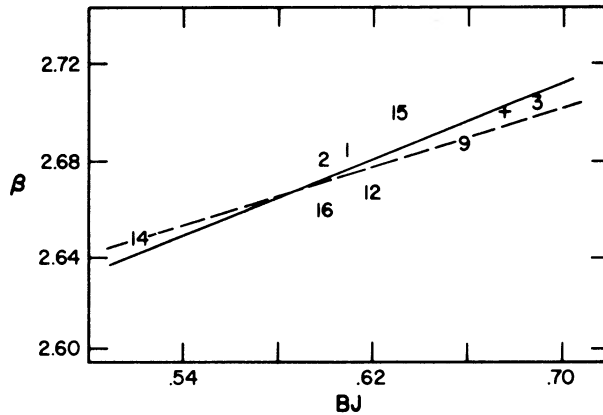


FIG. 8.—Relation between  $\beta$ -index and BJ; the observed BJ compared with Crawford's  $\beta$ -index. *Cross*, the B5 V star  $\kappa$  Hya. Two lines show the possible relations: *solid line*,  $\delta BJ = 2.5 \delta \beta$ ; *broken line*,  $\delta BJ = 3.3 \delta \beta$ .

nor with the theory. Guthrie (1963) reported, of cluster-member B stars, that the excess of  $\beta$ -index in the  $[\beta, (U - B)_0]$ -diagram shows a correlation with  $v \sin i$  which roughly matches the theory. Figure 8 relates our BJ to the  $\beta$ -index observed by Crawford (1958) and adopted by Guthrie (1963). The  $\beta$ -index of  $\eta$  UMa was converted from the  $\Gamma$ -index obtained by Bappu *et al.* (1962) ( $\beta = 3.1568 - 0.00227 \Gamma$  according to Guthrie 1963). The rotational effect in the  $\beta$ -index was transformed into that in the BJ by making use of an approximate relation  $\delta BJ \simeq 2.5 \delta \beta$  (Fig. 8); it appears in Figure 7, illustrating the observations by Guthrie (1963) and also the prediction of Hardorp and Strittmatter (1968*b*). Even when the ambiguities of the observed values are taken into account, some rapid rotators observed definitely show an excess in BJ which is comparable with a gravity effect of  $\delta \log g = 1$ . The model atmospheres for  $\log g = 4.0$  for the effective

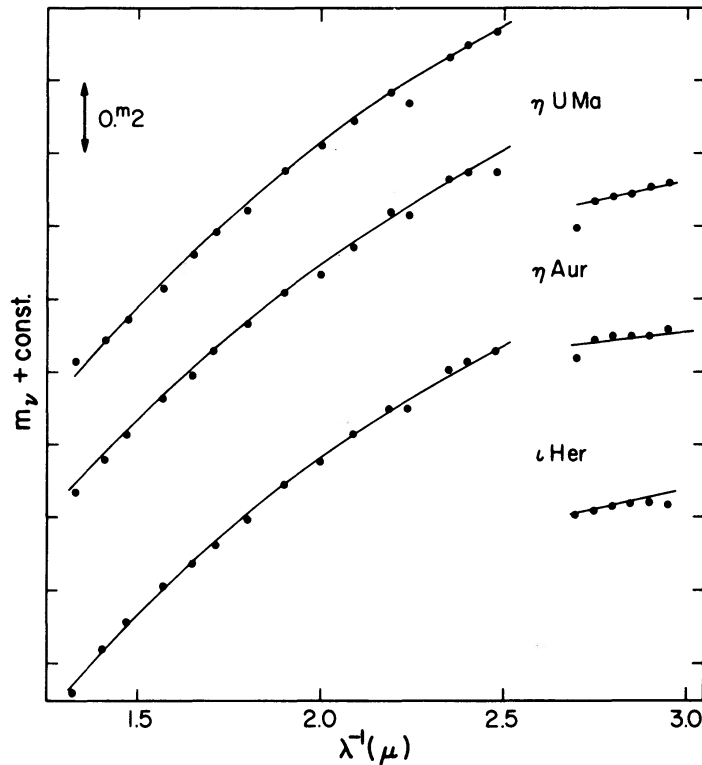


FIG. 9.—Comparison between observed and theoretical continua. Curves are model continua calculated by Mihalas;  $\eta$  UMa:  $\theta_e = 0.28$ ,  $\log g = 4.5$ ;  $\eta$  Aur:  $\theta_e = 0.30$ ,  $\log g = 4.0$ ;  $\iota$  Her:  $\theta_e = 0.28$ ,  $\log g = 3.5$ .

temperatures given in Table 4 are, consequently, expected to give smaller BJ's and weaker Balmer lines than observed for these objects. If the effect is due to a dispersion in the surface gravity, then the observed correlation with  $v \sin i$  is remarkable. In analyses of high-dispersion spectra, the consistency between the strengths of Balmer lines and other spectroscopic characteristics should be carefully investigated.

Finally, the quality of the fit between the observed and the model continua is shown in Figure 9. Values of  $\log g = 3.5$  and  $\theta_e = 0.28$  were adopted for  $\iota$  Her;  $\log g = 4.0$  and  $\theta_e = 0.30$  for  $\eta$  Aur; and  $\log g = 4.5$  and  $\theta_e = 0.28$  for  $\eta$  UMa; the fit is satisfactory.

We wish to thank Drs. J. B. Oke and R. E. Schild for valuable discussions and information, and Dr. D. S. Hayes for his kind comments. We are indebted to Dr. and Mrs. Jesse L. Greenstein for reading the manuscript.

## REFERENCES

- Adams, T. F., and Morton, D. C. 1968, *Ap. J.*, **152**, 195.  
 Bahner, K. 1963, *Ap. J.*, **138**, 1314.  
 Bappu, M. K. V., Chandra, S., Sanwal, N. B., and Sinval, S. D. 1962, *M.N.R.A.S.*, **123**, 521.  
 Baschek, B., and Oke, J. B. 1965, *Ap. J.*, **141**, 1404.  
 Brown, R. Hanbury, Davis, J., Allen, L. R., and Rome, J. N. 1967, *M.N.R.A.S.*, **137**, 393.  
 Crawford, D. L. 1958, *Ap. J.*, **128**, 185.  
 Guthrie, B. 1963, *Pub. Roy. Obs. Edinburgh*, **3**, 84.  
 Hardorp, J., and Scholz, M. 1968, *Zs. f. Ap.*, **69**, 350.  
 Hardorp, J., and Strittmatter, P. A. 1968a, *Ap. J.*, **151**, 1057.  
 ———. 1968b, *ibid.*, **153**, 465.  
 Hayes, D. 1967, unpublished thesis, University of California, Los Angeles.  
 Heintze, J. R. W. 1968, *B.A.N.*, **20**, 1.  
 ———. 1969, *ibid.*, **20**, 154.  
 Hoffleit, D. 1964, *Catalogue of Bright Stars* (3d ed.; New Haven, Conn.: Yale University Observatory).  
 Johnson, H. L., Mitchell, R. I., Iriarte, B., and Wisniewski, W. Z. 1966, *Comm. Lunar and Planet. Lab.*, **4**, 99.  
 Jugaku, J., and Sargent, W. L. W. 1968, *Ap. J.*, **151**, 259.  
 Kodaira, K., and Scholz, M. 1970, to be published.  
 Kraft, R. P., and Wrubel, M. 1965, *Ap. J.*, **142**, 703.  
 Mihalas, D. 1965, *Ap. J. Suppl.*, **9**, 321.  
 ———. 1966, *ibid.*, **13**, 1.  
 Mihalas, D., and Morton, D. C. 1965, *Ap. J.*, **142**, 253.  
 Mihalas, D., and Stone, M. E. 1968, *Ap. J.*, **151**, 293.  
 Moore, J. H., and Neubauer, F. J. 1948, *Lick Obs. Bull.*, **20**, 1.  
 Oke, J. B. 1964, *Ap. J.*, **140**, 689.  
 Slettebak, A., and Howard, R. F. 1955, *Ap. J.*, **121**, 102.  
 Strittmatter, P. A. 1966, *Ap. J.*, **144**, 430.  
 Strittmatter, P. A., and Sargent, W. L. W. 1966, *Ap. J.*, **145**, 130.  
 Sweet, P. A., and Roy, A. E. 1953, *M.N.R.A.S.*, **133**, 701.  
 Whiteoak, J. B. 1966, *Ap. J.*, **144**, 306.  
 Whitford, A. E. 1958, *A.J.*, **63**, 201.  
 Wolff, S. C., Kuhl, L. V., and Hayes, D. 1968, *Ap. J.*, **152**, 871.

